The 11th Canadian Conference on Earthquake Engineering
Canadian Association for Earthquake Engineering

PERFORMANCE OF RETROFITTED SQUAT CONCRETE SHEAR WALLS

W. Leonardo CORTÉS-PUENTES
PhD Candidate, Dept. of Civil Engineering, University of Ottawa, Canada
wcort032@uottawa.ca

Dan PALERMO
Associate Professor, Dept. of Civil Engineering, York University, Canada
dan.palermo@lassonde.yorku.ca

ABSTRACT: Two, 1/3rd-scale, squat concrete shear walls were tested under reverse cyclic loading with the objective to better understand the behaviour of nonseismically designed walls and to investigate the effect of various retrofitting methodologies. The design of the walls was in accordance with the 1965 edition of the NBCC to represent concrete design and construction practices prior to the implementation of seismic requirements in the 1970s. Normal and low concrete strengths were used to replicate typical materials used in older construction. The wall with normal concrete strength experienced rocking along with sliding shear at the base, while the wall with lower concrete strength was controlled by shear deformations and wide spread diagonal shear cracking. The test results highlight the necessity to improve the response of older walls to meet modern seismic demands. Numerical simulations were performed to assess the effect of seismic retrofit strategies on the response of squat concrete walls, including: steel plates, fiber reinforced polymer (FRP) sheets, and shape memory alloy (SMA) bracing. Results from the analyses indicate that retrofitting methods with steel, FRP, and SMA have the potential to improve the seismic response of squat concrete walls.

1. Introduction

Squat reinforced concrete shear walls are stiff structural elements that find applications in various low-rise structures such as parking and residential buildings, podiums of high-rise buildings, schools, hospitals, and bridges. Due to their high stiffness, squat shear walls are very efficient at controlling lateral deformations. However, when not properly designed for the seismic demands prescribed by modern codes, squat shear walls may experience undesirable damage and failure. Shear deformations and shear sliding in squat shear walls reduce the energy dissipation capacity and ductility, which may trigger brittle failure and collapse. In response to these deficiencies, retrofitting techniques incorporating steel plates, FRP sheets, or novel applications of shape memory alloys (SMAs) have materialized as effective means for improving seismic performance. However, research on these retrofitting techniques on squat reinforced concrete shear walls is limited, specifically the latter.

Retrofitting techniques in the form of external steel plates and FRP sheets have previously been investigated to improve the seismic response of squat reinforced concrete shear walls. Bolted steel plates as a retrofit can improve strength, ductility, and energy dissipation capacities (Tagdhi et al., 2000). This methodology, however, results in extensive damage and permanent residual deformations caused by yielding of the internal reinforcing steel and retrofitting steel plates. FRP Sheets can provide enhanced strength improvements provided adequate bonding and anchoring of the FRP (Lombard et al., 2000). However, premature debonding of FRP sheets results in limited enhancement in strength, ductility and energy dissipation capacities (Hsiao et al., 2008). The response of FRP is linear; therefore, the contribution to energy dissipation is minimal. Despite the strength improvement provided by the FRP, walls retrofitted with FRP are characterized with significant shear cracking and residual deformations (Lombard et al., 2000;

Hsiao et al., 2008). The use of SMA bars for retrofitting squat concrete shear walls has been shown to improve the strength capacity (Effendy et al., 2006). However, if the SMA bars are subject to small deformations typical of squat walls, the full benefit of the energy dissipation, recentering and recovery of plastic deformation capacities of the SMA is not realized. Although external retrofitting methods with steel, FRP, and SMA have been investigated, further experimental and numerical studies are required to assess the application and effectiveness of these methods on squat concrete shear walls.

2. Testing of Squat Concrete Shear Walls

2.1. Test Specimens

The walls tested in this research were 1/3rd-scale of a 6000 mm x 6000 mm x 300 mm prototype wall designed with minimum reinforcement (0.21% and 0.18% horizontal and vertical reinforcement ratio, respectively) according to the NBCC-1965 (NRC, 1965). Based on the assumption of similar material properties between the prototype and specimen walls, the following scaling factors were calculated: geometric factor of 1/3, force factor of 1/9, stress factor of 1, and reinforcement ratio factor of 1. Scaling of the prototype wall resulted in 2000 mm x 2000 mm x 100 mm wall specimens (SQ1 and SQ1a) with web reinforcement of 6-9.5 mm-diameter horizontal reinforcing bars (reinforcement ratio of 0.21%) and 5-9.5 mm-diameter vertical reinforcing bars (reinforcement ratio of 0.18%) (Fig. 1(a)).

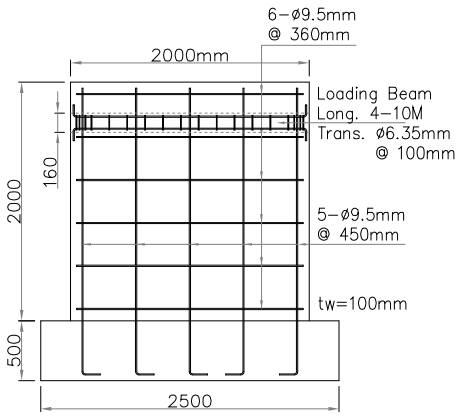

(a)

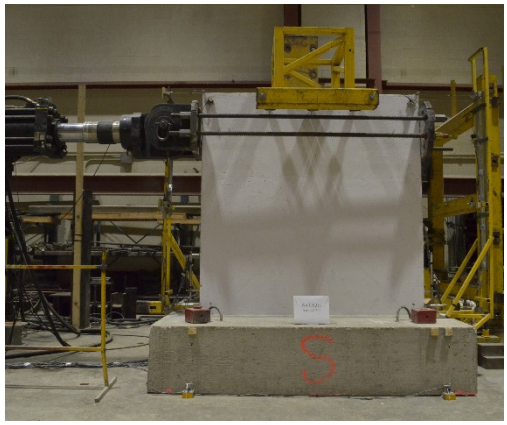

(b)

Fig. 1 – Wall Specimens: (a) Reinforcement Layout; and (b) Testing Setup

The calculated strength capacity of the wall specimens was 115 kN. Walls SQ1 and SQ1a represent typical lightly reinforced walls that are prone to failure associated with shear (sliding and diagonal cracking). The concrete used to construct Wall SQ1 had compressive strength of 22.5 MPa and the steel had yield strength of 495 MPa. Wall SQ1a was designed with the same geometry and reinforcement layout as Wall SQ1 but with lower concrete compressive strength (9.5 MPa). Both walls, SQ1 and SQ1a, were constructed with heavily reinforced 500 mm-thick foundation blocks and 100 mm x 160 mm embedded loading beams (Fig. 1(a)).

2.2. Loading Protocol

Lateral loading of the walls consisted of a reverse cyclic protocol with two repetitions at each displacement level following recommendations of FEMA 461 (FEMA, 2007). The loads were applied with a 1000 kN capacity actuator placed at 1660 mm from the base of the wall (Fig. 1(b)). Loading commenced with cyclic amplitude to 0.25 mm displacement. In the pre-damage stage (prior to the yield displacement, Δy), the cyclic amplitudes were increased by a factor of 2. In the damage stage (between yielding, Δy, and the target maximum displacement, Δm), the cyclic amplitudes were increased by a factor of 1.4. Beyond the target maximum displacement, the cyclic amplitudes were increased by a constant increment of 0.25Δm until failure. Yield displacement and maximum target displacement at the top of the wall were 3 mm and 40 mm, respectively; established using preliminary analyses with Program VecTor2. The axial load of the prototype wall was less than 2 % of $A_g f'_c$. No axial loading was imposed on the wall test specimens, given the low level of axial loading on the prototype walls.

2.3. Wall SQ1

The low percentages of reinforcement in Wall SQ1 limited the contribution of the steel to the flexural and shear capacities. This resulted in concentrated damage at the base of the wall in the form of shear cracking and shear sliding. Given the localized damage, the wall experienced rocking until significant sliding shear and steel rupture reduced the strength capacity. The lateral load-top displacement response illustrates a highly pinched behaviour dominated by shear degradation due mainly to localized cracking at the base and sliding shear (Fig. 2). The wall behaved linearly until cracking at 0.5 mm. The corresponding strength was 65 kN. Initial cracking resulted in significant loss of stiffness. Yielding was achieved at approximately 3 mm as indicated by the change of slope of the hysteretic cycles between 3 mm and 4 mm. Beyond 3 mm of displacement, the load was sustained, following a near-constant plateau with a marginal post-yield stiffness. At 3 mm, the strength was 100 kN in the positive direction and 90 kN in the negative direction. With increasing displacements, a localized wide cracked formed at the base of the wall, which promoted sliding with respect to the foundation. Due to an instrumentation error, the wall was loaded asymmetrically in all subsequent load stages beyond 4 mm of lateral displacement. This resulted in recorded displacements that did not necessarily correspond with the intended targeted displacements. This became evident after constructing the lateral load-top displacement response. During loading to the intended target displacement of 5 mm, the first repetition resulted in recorded displacements of +6.3 mm/-9.6 mm. During this cycle, maximum strengths of 115 kN and 105 kN were recorded in the positive and negative directions, respectively. During loading to the intended target displacement of 8 mm, the first repetition resulted in recorded displacements of +7.1 mm/-16 mm. During the second repetition of loading, cracking at the right end of the wall did not fully close while pushing the wall in the positive direction, limiting the strength capacity. During loading to the intended target displacement of 10 mm, a substantial difference in lateral strength between the positive and negative cycles was recorded. During this cycle, the strength capacities were 45 kN and 100 kN in the positive and negative directions, respectively. However, the actual recorded displacements were +4.6 mm/-17.8 mm. Therefore, it was realized that the full capacity of the wall was not yet captured. As a result, an additional cycle to 50 mm was imposed on the wall to capture the post-peak behaviour. A sudden drop in the strength was recorded at +37 mm of displacement, after sustaining peak strength of 145 kN. The drop in lateral load capacity coincided with rupturing of one of the outer reinforcing bars. In the negative direction, the peak strength of was 115 kN. Two drops at -46.3 mm and -58.2 mm were associated with rupturing of two additional reinforcing bars near the right end of the wall. The maximum-recorded width of the crack at the base of the wall was 17 mm and 24 mm, corresponding to lateral displacements of 28 mm and -39 mm, respectively. It is probable that debonding of the vertical reinforcement near the base of the wall played a significant role in the response of Wall SQ1, specifically during the cycle to 50 mm. The response of the wall was dominated by rigid body motion along the horizontal crack at the base of the wall. Therefore, the crack opening would reasonably be expected to be similar to the lateral displacement at the top of the wall. This would result in a crack width of approximately 40 mm at the base, corresponding to the approximate displacement at peak lateral strength capacity. At this level of localized crack opening, the reinforcement should have fractured.

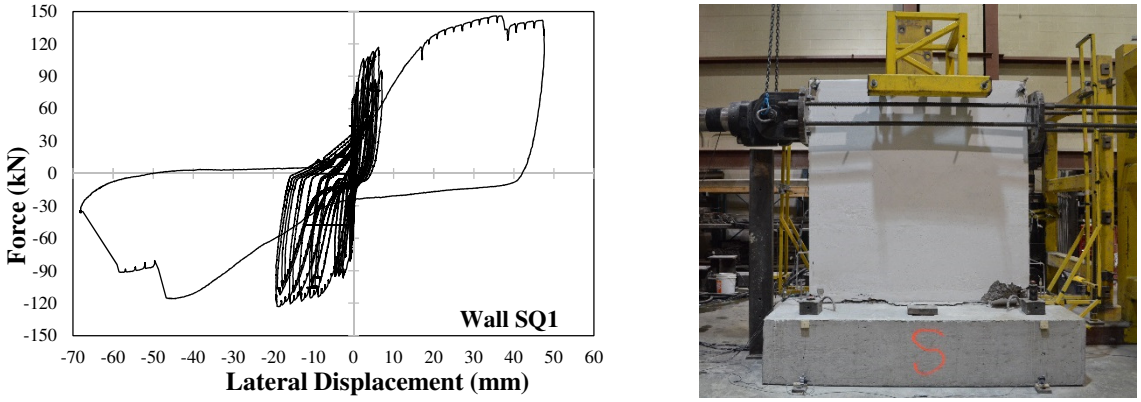

Fig. 2 – Response of Wall SQ1: (a) Force-Displacement Response; and (b) Damage at Ultimate

2.4. Wall SQ1a

Wall SQ1a responded with satisfactory ductility (large displacement capacity after yielding), but displayed significant stiffness and strength degradation as well as pinching due to diagonal shear cracking and sliding (Fig. 3). First cracking was observed at +0.6 mm of top displacement, corresponding to lateral strength of 45 kN. The width of the horizontal crack that formed at the base of the wall was 0.2 mm. After first cracking, damage of concrete gradually affected the stiffness and strength of the wall. A change in stiffness was evident in the envelope of the lateral load-top displacement response at 2.4 mm, indicating that yielding of the vertical reinforcement had initiated. At 2.4 mm of displacement, the strength of the wall was 86 kN in the positive direction and 95 kN in the negative direction. With increasing load, additional cracks surfaced on the wall; the majority were diagonal in direction. The lateral strength of the wall increased approximately 15% from 2.4 mm to 7 mm of displacement. Thereafter, the strength was sustained to failure. Shear-related mechanisms were significant in the response of the wall as indicated by the extensive diagonal cracking and pinching of the hysteretic response. With increasing displacements, the wall experienced additional damage and; therefore, degradation of the response was augmented. The wall experienced reduced lateral stiffness and strength when subjected to the second repetitions of the cycles due to damage experienced during the first repetitions (development of new cracks and opening of existing cracks). The difference in response between first and second repetitions was more evident at displacement levels near failure. At 32 mm of displacement, the wall reached its peak strength capacity of 118 kN. In the post-peak, stiffness and strength degradation was evident (Fig. 3(a)). Failure of the wall occurred at 40 mm of displacement. The lateral strength of the wall at 40 mm was 97 kN in the positive direction and 101 kN in the negative direction. Approximately 30% of the lateral capacity was lost during the second repetition to 40 mm; the average strength during the second repetition to 40 mm of displacement was 70 kN. Heavy damage was evident in the wall, confirming failure. While pulling the wall to the negative direction during the second repetition to 40 mm, a vertical reinforcing bar near the right end of the wall ruptured, causing a sudden drop of strength of approximately 25 kN. The combined size of the two lower cracks, as measured by an LVDT, at the end of the wall (horizontal crack along the base and first diagonal crack at 200 mm from the base) was 15 mm at the left end and 25 mm at the right end. Note that at 40 mm, damage of the lower corners included cracking, crushing of concrete, and buckling of the vertical bars. An additional cycle to 50 mm was imposed, and the strength decreased to 30 kN in the positive direction and 38 kN in the negative direction. Residual strength of only 15 kN was recorded during the second repetition to 50 mm.

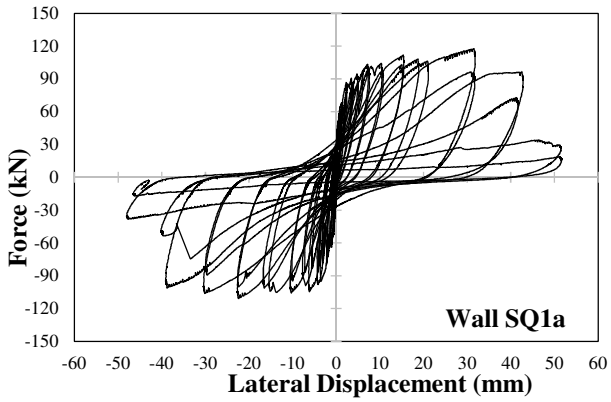

(a)

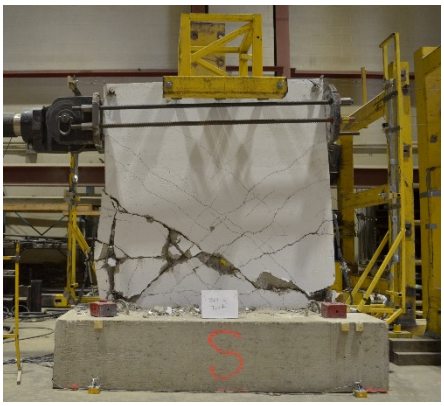

(b)

Fig. 3 – Response of Wall SQ1a: (a) Force-Displacement Response; and (b) Damage at Ultimate

2.5. Discussion

Walls SQ1 and SQ1a were governed by shear-related mechanisms. However, the behaviour of the walls significantly differed due to the difference in concrete strength (22.5 MPa for SQ1 and 9.5 MPa for SQ1a). Wall SQ1 experienced rocking due to a major crack at the base (at the intersection with the foundation block). This large crack promoted rocking and sliding shear as indicated by the pinching of the hysteretic response. Wall SQ1a was controlled by shear distortion caused by diagonal cracking distributed from the base to the loading height. The diagonal cracks along with sliding of the adjacent concrete resulted in pinching of the response. Although Wall SQ1 and Wall SQ1a exhibited different cracking patterns, degradation of their respective behaviours was affected similarly by the shear deformations. First cracking

in both walls was observed at similar displacements (0.5 mm for Wall SQ1 and 0.6 mm for Wall SQ1a), but propagated differently with increased lateral displacements. Cracking and shear-related mechanisms affected the stiffness and strength of the walls. The degradation was mainly due to the lack of recovery capacity to close the cracks. Degradation of the response increased due to the permanent deformations experienced by the vertical reinforcing bars in the post-yield range. The walls experienced similar ductility, and failure included crushing and spalling of concrete and rupturing of the vertical reinforcing steel. Strength of Wall SQ1a was comparable to that of Wall SQ1 in the negative direction. However, it was approximately 20% higher for Wall SQ1 in the positive direction. Differences in strength were mainly due to the different concrete strengths used in the construction of the walls.

3. Numerical Simulation of Retrofitting Methods

Wall SQ1 was simulated with the nonlinear finite element program VecTor2 to predict the reverse cyclic response of the original and retrofitted state of the wall. VecTor2 is based on the Modified Compression Field Theory (MCFT) and the Disturbed Stress Field Model (DSFM) and employs a smeared rotating crack approach to model cracked concrete. The program includes comprehensive constitutive models for concrete, reinforcing steel, FRP sheets, and superelastic SMA. Details of these models can be found elsewhere (Wong et al., 2013). Three additional walls, Wall SQ1STL (steel plate retrofit), Wall SQ1FRP (FRP sheet retrofit), and Wall SQ1SMA (SMA brace retrofit) were modelled to assess the seismic response of SQ1 after retrofitting. Important behavioural parameters, including strength capacity, ductility, and recentering capability were investigated. The retrofitting systems followed a diagonal layout to avoid additional shear stresses associated with increases in flexural response. Three different retrofitting anchoring techniques were studied: perfect bond for the steel plates, partial bond for the FRP sheets, and no bond for the SMA braces. Note that only the ends of the SMA braces were rigidly attached at the base and top of the shear wall; therefore, the remainder of the braces was not connected to the wall. Steel and FRP retrofitting methods conformed to techniques previously tested and reported by other researchers (Tagdhi et al., 2000 and Hsiao et al., 2008). The SMA retrofitting simulated tension-only SMA braces where the length of the SMA is optimized to obtain a hybrid system with substantial energy dissipation and marginal residual deformation. The nonlinear finite element methods employed herein have been successfully utilized to predict the reverse cyclic response of retrofitted concrete shear walls, including externally bolted steel plates and externally bonded FRP sheets (Cortés-Puentes and Palermo, 2012a).

Retrofitting of Wall SQ1 was intended to increase the strength of the original wall by approximately 60%. The target strength was based on a seismic assessment conducted on original and retrofitted prototype walls (Cortés-Puentes and Palermo, 2012b) to satisfy seismic requirements prescribed by the 2010 edition of the NBCC (NRC, 2010). Design of the retrofitting systems was based on the yield strength of the retrofitting materials with the exception of the FRP sheets. Retrofitting with FRP was designed based on 50% of the ultimate strength of the FRP sheets. Therefore, the three retrofitting systems were expected to develop similar axial force of 90 kN.

3.1. Modelling

Modelling of Wall SQ1 consisted of four reinforced concrete zones: one corresponding to the web, one for the foundation block, and two for the embedded loading beam at 1660 mm from the base (Fig. 4(a)). The web consisted mainly of 100 mm-thick, 90 mm x 90 mm rectangular concrete elements. The horizontal and vertical internal reinforcement was modelled with discrete one-dimensional truss elements. Concrete and steel were modelled with the properties obtained in the laboratory: concrete compressive strength of 22.5 MPa, steel yield stress of 495 MPa and corresponding yield strain of 0.3%, and steel ultimate stress of 735 MPa and corresponding strain of 16%.

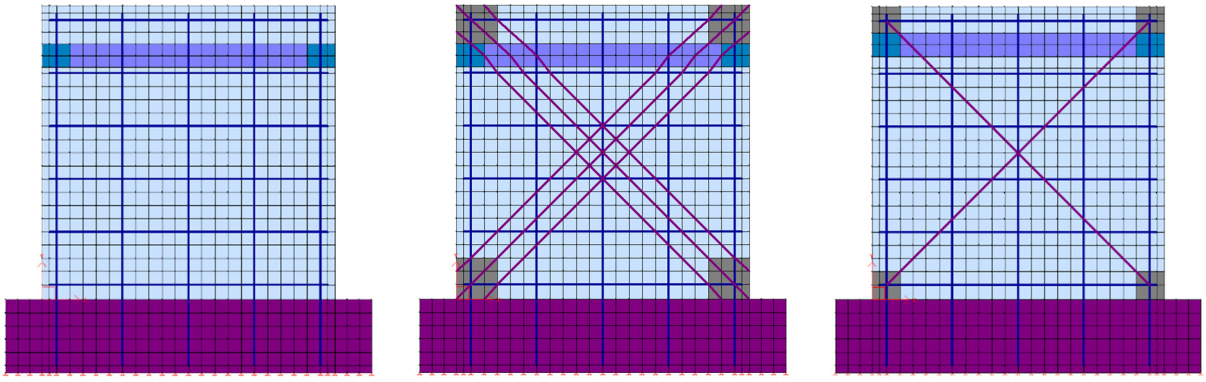

Fig. 4 – Modelling of Shear Walls: (a) SQ1; (b) SQ1STL and SQ1FRP; and (c) SQ1SMA

The steel plates in the retrofit of Wall SQ1STL was modelled with steel truss elements, which were directly connected to the concrete rectangular elements to simulate perfect bonding (steel truss elements shared nodes with the rectangular concrete elements) (Fig. 4(b)). Each diagonal steel plate consisted of three lines of truss elements, each one with a cross-sectional area of 120 mm^2. The steel plates had a yield stress of 250 MPa and an ultimate stress of 375 MPa. Similar to the steel plates, the diagonal externally bonded FRP sheets (Wall SQ1FRP) were modelled with three lines of truss elements with total cross sectional area of 210 mm^2, ultimate stress of 876 MPa and modulus of elasticity of 72 400 MPa (Fig. 4(b)). The truss elements were connected to the concrete elements with bond-link elements, which were assigned a bilinear bond stress-slip relationship with maximum slip stress of 3.93 MPa and corresponding slip displacement of 0.035 mm to simulate the bonding interface between concrete and FRP. The stress and slip parameters followed a formulation for externally bonded carbon FRP based on the fracture energy method (Sato and Vecchio, 2003). The SMA braces in the retrofit of Wall SQ1SMA were simulated with single truss elements with cross-sectional area of 252 mm^2 and length of 2540 mm. The length of the truss elements accounted for the length of the adjoining rigid steel elements (Fig. 4(c)). The truss elements were connected to opposite corners at the base and top of the wall. Properties of the SMA elements corresponded to a flag-shape stress-strain relationship obtained from cyclic tests of tension-only SMA braces: yield stress of 365 MPa, modulus of elasticity of 73 000 MPa, ultimate stress of 528 MPa, and ultimate strain of 1.63% (Fig. 5). The SMA braces consist of tension-only SMA links coupled with rigid steel elements. The length of the SMA links was designed to ensure yielding (forward transformation of the SMA) and to sustain maximum deformation of 35 mm (5.5% strain). Exceeding the yield point permits the deformation recovery action of the brace, while not exceeding the strain limit of 5.5% permits reusability of the brace. All the models for the retrofitted walls included heavily reinforced zones at the top and bottom corners of the walls to simulate anchoring of the retrofitting systems (Fig. 4). Original and retrofitted walls were analyzed with incremental reverse cyclic lateral displacements, starting with 0.25 mm, applied at the loading beam. The loading protocol consisted of two repetitions for each displacement cycle.

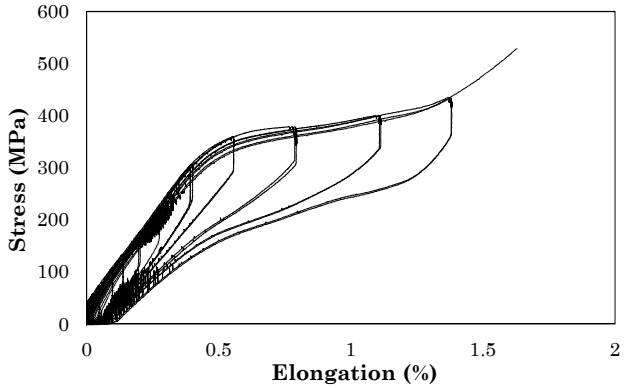

Fig. 5 – Response of Tension-Only SMA Brace

3.2. Predicted Response

The analysis of SQ1 predicted a major horizontal crack at the base of the wall and the absence of damage in other locations due to the limited tensile force provided by the vertical reinforcement (Fig. 6(b)), which was not sufficient to fracture the concrete, resulted in rocking of the wall. This response is typical of lightly reinforced concrete squat walls. Damage of the concrete (cracking and sliding at the base) caused stiffness and strength degradation between repetitions of loading to the same displacement levels (Fig. 6(a)). The analysis predicted lateral strength capacity of 136 kN, which was sustained up to 20 mm of displacement. Failure of the wall occurred due to crushing of concrete and rupturing of vertical reinforcing bars near the bottom corners of the wall. Rupture of steel occurred at 26 mm of displacement, while crushing of concrete initiated at 15 mm. Prior to failure, the residual lateral displacement of Wall SQ1 was 16 mm. While the predicted crushing of concrete was in agreement with the observed test behaviour, the ultimate displacement corresponding to rupture of steel was not. The internal reinforcement was assumed perfectly bonded, which resulted in premature rupturing of the vertical reinforcing steel bars. The hypothesized debonding of the vertical reinforcement discussed in Section 2.3, resulting in increased lateral displacements, was not captured with this model.

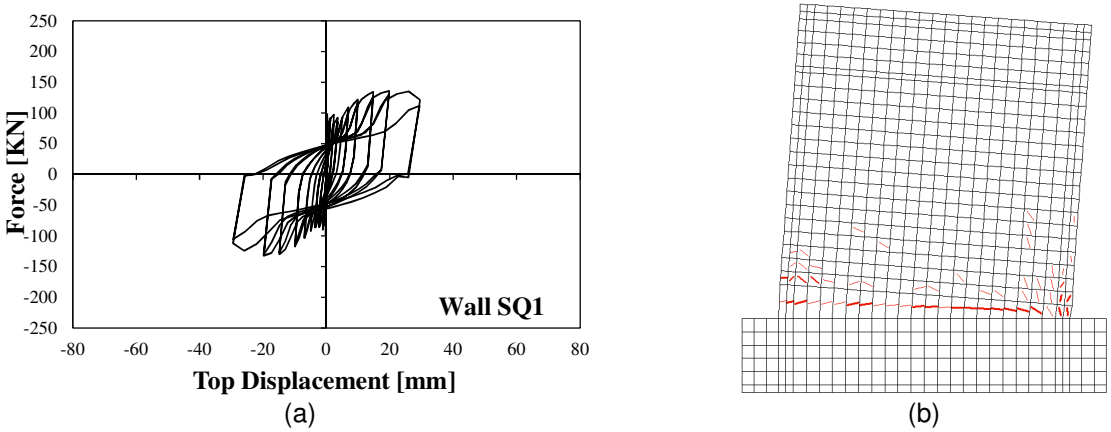

Fig. 6 – Response of Wall SQ1: (a) Force-Displacement Response; and (b) Damage at 20 mm

The numerical analysis of Wall SQ1STL predicted peak lateral strength capacity of 239 kN and maximum displacement of 70 mm (Fig. 7(a)). Wall SQ1STL responded primarily in flexure with concrete damage throughout the wall (Fig. 7(b)). The predicted damage included diagonal shear cracking in addition to flexural cracking, specifically near the steel plates. In the post-yield range, the analysis predicted some strength degradation between first and second repetitions to the same displacement level, which was less in comparison to the original wall. Residual displacements of 16 mm and 48 mm at 20 mm and 60 mm of lateral displacement, respectively, were predicted. The failure mechanism consisted of crushing of concrete at the toes of the walls followed by rupturing of the vertical reinforcing steel. A drop of strength of approximately 20 kN was predicted at 36 mm due to loss of compression capacity of the lower corners of the wall. Rupture of the vertical reinforcing bars was predicted at 70 mm. Note that buckling of the plates was not explicitly modelled due to the assumed closely spaced connections between the steel plates and concrete elements.

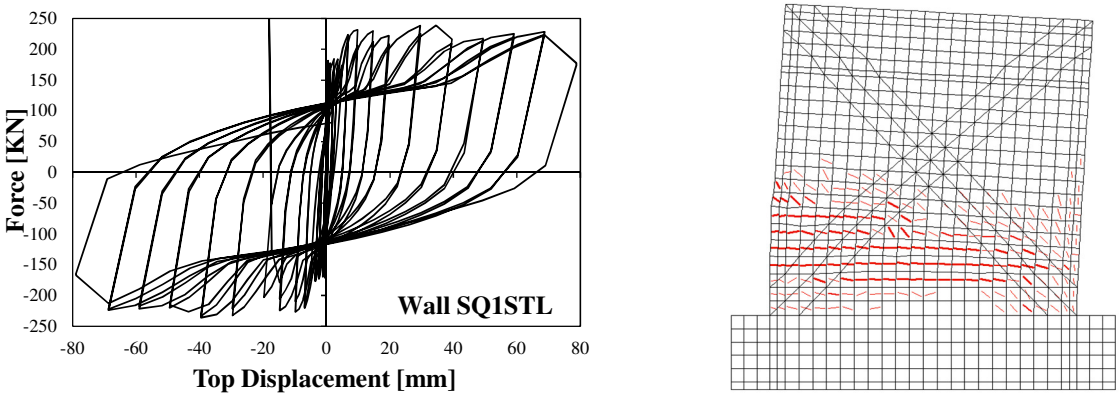

Fig. 7 – Response of Wall SQ1STL: (a) Force-Displacement Response; and (b) Damage at 20 mm

The predicted ultimate lateral strength of Wall SQ1FRP was 243 kN, corresponding to an ultimate displacement of 20 mm (Fig. 8(a)). The retrofit system with FRP improved the strength capacity of the wall, but reduced the ductility. The linear behaviour of the FRP resulted in rapid increase of the strength that promoted brittle damage of the concrete. However, the FRP improved the recentering of the wall by bridging the concrete cracks, specifically during unloading. Due to the partial bond of the FRP, transfer of the axial forces within the retrofitting material to the concrete was concentrated near the base of the wall. Furthermore, degradation of the bonding stress of the FRP induced softening of the response beyond 2 mm of displacement (Fig. 8(a)). Wall SQ1FRP exhibited high initial stiffness and strength similar to the original wall. As a result, damage of the wall and rocking was similar to that predicted for Wall SQ1. A major horizontal crack was localized slightly above the lower anchoring zones (Fig. 8(b)). The FRP sheets contributed to reduce the stiffness and strength degradation observed in Wall SQ1. Failure due to rupturing of the vertical reinforcing bars was predicted at 20 mm of displacement during loading in the pushing direction to 24 mm. Prior to failure, the residual displacement was 12 mm.

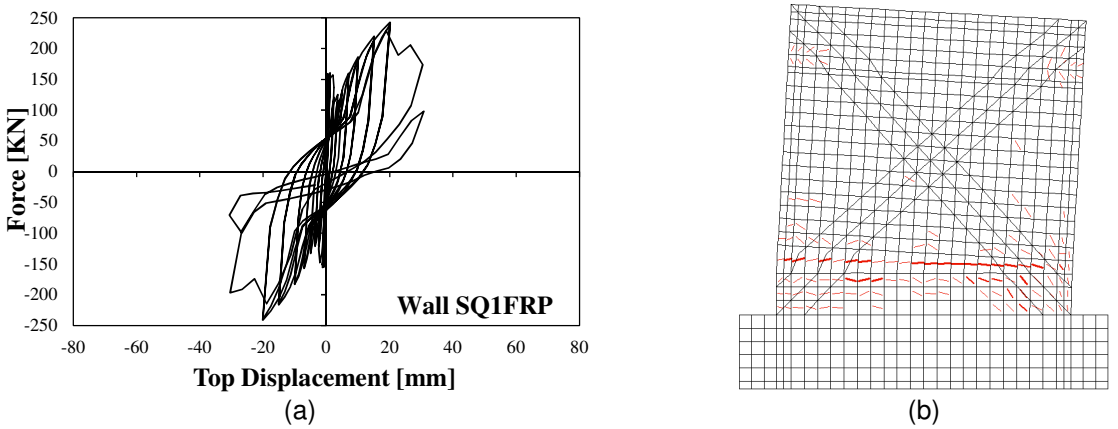

Fig. 8 – Response of Wall SQ1FRP: (a) Force-Displacement Response; and (b) Damage at 20 mm

The predicted response of Wall SQ1SMA was more flexural with less stiffness degradation in comparison to Wall SQ1 (Fig. 9(a)). Flexural cracks were predicted at the lower third of the wall (Fig. 9(b)). The SMA braces increased the strength capacity of the wall to 235 kN as well as the maximum displacement to 58 mm. The reduction of the stiffness degradation and the shape of the loading branches of the hysteretic response indicated improvements in crack closure, which in turn, improved the shear response. Furthermore, the SMA braces absorbed part of the shear demand and alleviated the shear stresses in the concrete. As a result, the wall exhibited marginal strength degradation between repetitions to the same displacement amplitudes. An important aspect of the retrofitting scheme was the recentering capability. The SMA braces significantly reduced the residual displacement. The residual displacement was 9 mm and 26 mm at 20 mm and 58 mm of lateral displacement, respectively. The recentering capabilities promoted a

more stable cyclic response with good energy dissipation capacity, specifically for load repetitions to same displacements. Tensile forces carried by the retrofitting system resulted in additional compressive stresses and crushing of concrete in the lower corners of the wall that reduced the strength of the wall at 30 mm. Failure of the wall occurred at 58 mm due to rupturing of the vertical reinforcing bars located near the ends of the wall.

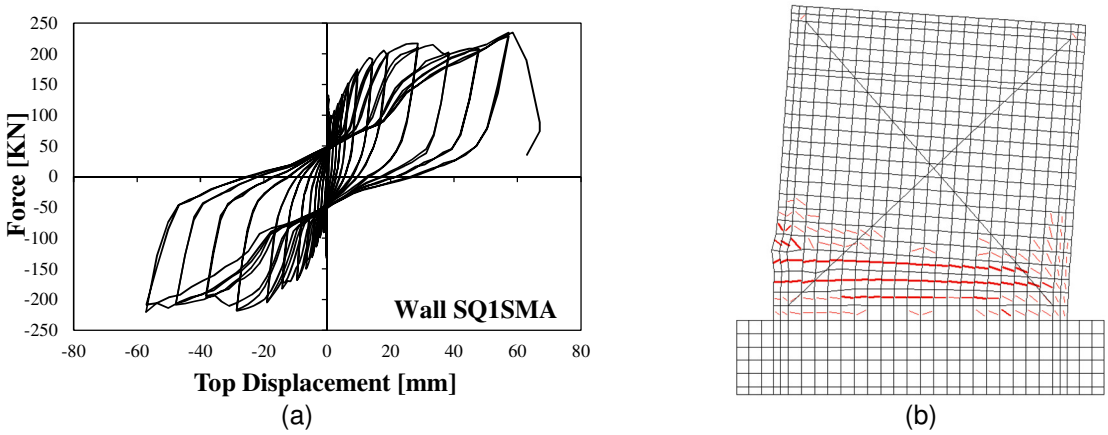

(a) (b)

Fig. 9 – Response of Wall SQ1SMA: (a) Force-Displacement Response; and (b) Damage at ultimate

3.3. Discussion

The three retrofitting methods simulated with the finite element method improved the behavioural response of Wall SQ1. The walls retrofitted with steel plates (SQ1STL) and SMA braces (SQ1SMA) improved the flexural response of Wall SQ1, while the wall retrofitted with FRP resulted in rocking behaviour similar to Wall SQ1. Strength of Wall SQ1 was similarly increased to approximately 240 kN with the application of the three retrofitting systems (approximately 75% increase). All three retrofitting systems reduced the stiffness and strength degradation of the original wall, specifically between the two repetitions to the same displacement amplitudes. The response of the retrofitted walls significantly differed in term of displacement capacity. The walls retrofitted with steel plates and SMA braces sustained maximum displacements of approximately 70 mm and 60 mm, respectively, while the wall retrofitted with FRP experienced maximum displacement of 20 mm (similar to that predicted for the original wall). The results indicated that the steel plate and SMA brace methods improved the ductility of Wall SQ1. Perfect bonding of the steel plates and the anchors of the SMA braces permitted satisfactory force transfer between the retrofitting system and the concrete, which promoted flexural behaviour and, therefore, more ductility. The wall retrofitted with FRP sheets did not sustain the peak lateral load experienced at 20 mm due to the linear response of the FRP sheets and the partial bonding condition. Bonding of the retrofitting systems along with the stress-strain relationship of the retrofitting materials affected the stiffness of the walls, specifically before achieving the peak lateral strength. The wall retrofitted with the steel plates rapidly reached peak strength (at 10 mm), while the peak strength was delayed in walls retrofitted with FRP (at 20 mm) and SMA (at 30 mm). Residual deformation was also affected by the stress-strain response of the retrofitting materials. At 20 mm of displacement, retrofitting with the steel plates resulted in same residual displacement as that predicted for the original wall (16 mm), while retrofitting with FRP sheets and SMA braces reduced the residual displacement to 12 mm and 9 mm, respectively. Note that for larger displacements, the SMA retrofitting system maintained its recovery capabilities. At ultimate state, the analyses predicted residual displacements of 26 mm and 50 mm for the walls retrofitted with steel plates and SMA braces, respectively.

4. Conclusions

This paper presented experimental results from testing two large-scale specimens with the same geometry but different concrete strengths to understand the reverse cyclic behaviour of nonseismically designed squat concrete shear walls. Shear-related mechanisms highly affected the response of the walls. The failure mechanisms were different due to differences in the concrete compressive strengths. The wall constructed with normal strength concrete (22.5 MPa) exhibited rocking behaviour due to a major horizontal crack at the base of the wall; while the wall with lower concrete strength (9.5 MPa) sustained shear distortion caused by distributed diagonal cracks. Based on the experimental results, numerical models were developed to

study three retrofitting methods: diagonal steel plates, diagonal FRP sheets, and diagonal SMA braces. The numerical study was conducted based on Wall SQ1 (wall constructed with normal concrete strength).

Nonlinear analyses demonstrated the capability of the three retrofitting methods to improve the reverse cyclic response of the original Wall SQ1. Retrofitting with steel plates and SMA braces improved flexural response and promoted additional distributed horizontal cracking, specifically within the lower portion of the wall near the base. Conversely, retrofitting with FRP sheets did not change the failure mode observed in the original wall (single crack at the base followed by rupturing of the vertical reinforcing steel). The three retrofitting systems increased the strength of the original wall approximately 75%. In terms of ductility, the steel plates and the SMA braces were more effective than the FRP sheets due to the stress-strain response of the materials and the anchoring and bonding conditions. While retrofitting with the steel plates and the SMA braces resulted in larger plastic displacement with improved ductile behaviour, retrofitting with the FRP sheets resulted in similar displacements to that of the original wall, which promoted brittle failure. Recentering was also dependant on the response of the retrofitting materials. The FRP and SMA retrofitting enhanced the recentering of the original wall (reduction of residual displacements of 25% and 44%, respectively), whereas the steel plate retrofitting resulted in same residual displacements as the original wall. Although the three retrofitting methods are suitable for strengthening seismically deficient squat concrete shear walls, the SMA brace method promises a more comprehensive retrofitting solution with significant enhancements of strength, ductility, and residual deformation.

5. Acknowledgements

The authors acknowledge the financial support from the Natural Sciences and Engineering Research Council (NSERC) through the Canadian Seismic Research Network (CSRN).

6. References

Cortés-Puentes W.L., and Palermo, D., “Modelling of reinforced concrete shear walls retrofitted with steel plates or FRP sheets”, *J. Struct. Eng.*, Vol. 138 No. 5, 2012a, pp. 602-612.

Cortés-Puentes, W.L. and Palermo, D., “Towards design of shear walls retrofitted with shape memory alloys”, *In: Proc. of 15th WCEE*, Lisbon, Portugal, September 2012b, pp. 1-10.

Effendy, E., Liao, W., Song, G., Mo, Y., and Loh, C., “Seismic behaviour of low-rise shear walls with SMA bars”, *In: Proc. of Earth & Space 2006*, Houston, Texas, March 2006, pp. 1-8.

FEMA, *FEMA 461: Interim Protocols for Determining the Seismic Performance Characteristics of Structural and Nonstructural Components*, Federal Emergency Management Agency, 2007.

Hsiao, F.P., Wang, J.C., and Chiou, Y.J., “Shear strengthening of reinforced concrete framed shear walls using CFRP strips”, *In: Proc. of 14th WCEE*, Beijing, China, October 2008, pp. 1-8.

Lombard, J., Lau, D.T., Humar, J.L., Foo, S., and Cheung, M.S., “Seismic strengthening and repair of reinforced concrete shear walls”, *In: Proc. of 12th WCEE*, Auckland, New Zealand: New Zealand Society for Earthquake Engineering, January 2000, paper 2032 pp. 1-8.

NRC, *National building code of Canada*, Associate committee on the national building code, National research council of Canada, Ottawa, ON, Canada, 1965.

NRC, *National building code of Canada*, Associate committee on the national building code, National research council of Canada, Ottawa, ON, Canada, 2010.

Sato, Y., and Vecchio, F.J., “Tension stiffening and crack formation in reinforced concrete members with fiber-reinforced polymer sheets.” *J. Struct. Eng.*, Vol. 129 No. 6, 2003, pp. 717–724.

Taghdi, M., Bruneau, M., and Saatcioglu, M., “Seismic retrofitting of low-rise masonry and concrete walls using steel strips”, *J. Struct. Eng.*, Vol. 126, No. 9, 2000, pp. 1017-1025.

Wong, P.S., Vecchio, F.J., and Trommels, H., *VecTor2 and Formworks user’s manual: second edition*, Dept. of Civil Engineering, University of Toronto, Toronto, Ontario, 2013.